

Muon spin relaxation studies of incommensurate magnetism and superconductivity in stage-4 $\text{La}_2\text{CuO}_{4.11}$ and $\text{La}_{1.88}\text{Sr}_{0.12}\text{CuO}_4$

A.T. Savici, Y. Fudamoto, I.M. Gat, T. Ito, M.J. Larkin, Y.J. Uemura¹
Department of Physics, Columbia University, New York, NY 10027, USA

G.M. Luke
Department of Physics and Astronomy, McMaster University, Hamilton, Ontario L8P 4N3, Canada

K.M. Kojin
Department of Superconductivity, Faculty of Engineering, University of Tokyo, 7-3-1 Hongo, Tokyo 113-8656, Japan

Y.S. Lee, M.A. Kastner
Department of Physics, MIT, Cambridge, MA 02139, USA

R.J. Birgeneau
Department of Physics, MIT, Cambridge, MA 02139, USA, and
Department of Physics, Univ. of Toronto, Toronto, Ontario M5S 1A7, Canada

K. Yamada
Institute for Chemical Research, Kyoto University, Uji, Kyoto 611-0011, Japan
(February 2, 2002)

We report muon spin relaxation (SR) measurements using single crystals of oxygen-intercalated stage-4 $\text{La}_2\text{CuO}_{4.11}$ (LCO :4.11) and $\text{La}_{1.88}\text{Sr}_{0.12}\text{CuO}_4$ (LSCO :0.12), in which neutron scattering studies have found incommensurate magnetic Bragg reflections. In both systems, zero-field SR measurements show muon spin precession below the Neel temperature T_N with frequency 3.6 MHz at $T = 0$, having a Bessel function line shape, characteristic of spin-density-wave systems. The amplitude of the oscillating and relaxing signals of these systems is less than half the value expected for systems with static magnetic order in 100 % of the volume. Our results are consistent with a simulation of local fields for a heuristic model with: (a) incommensurate spin amplitude modulation with the maximum ordered Cu moment size of $0.36 \mu_B$; (b) static Cu moments on the CuO_2 planes forming "islands" having typical radius $15 - 30 \text{ \AA}$, comparable to the in-plane superconducting coherence length; and (c) the measured volume fraction of magnetic muon sites V increasing progressively with decreasing temperature below T_N towards $V = 40 \%$ for LCO :4.11 and 18% for LSCO :0.12 at $T = 0$. These results may be compared with correlation lengths in excess of 600 \AA and a long range ordered moment of $0.15 - 0.05 \mu_B$ measured with neutron scattering techniques. In this paper we discuss a model that reconciles these apparently contradictory results. In transverse magnetic field SR measurements, sensitive to the in-plane magnetic field penetration depth λ_{ab} , the results for LCO :4.11 and LSCO :0.12 follow correlations found for underdoped, overdoped and Zn-doped high- T_c cuprate systems in a plot of T_c versus the superconducting relaxation rate ($T = 0$). This indicates that the volume-integrated value of n_s/m (superconducting carrier density / effective mass) is a determining factor for T_c , not only in high- T_c cuprate systems without static magnetism, but also in the present systems where superconductivity co-exists with static spin-

density-wave spin order.¹

I. INTRODUCTION

The interplay between superconductivity and magnetism is one of the central issues of high- T_c superconductivity (HTSC), which has been extensively studied both experimentally and theoretically.[1]. In particular, dynamic [2-8] and static [9-16] spin correlations with incommensurate wave vectors have been found by neutron scattering. These, as well as X-ray photoelectron studies [17-19], have been discussed in terms of a "stripe" modulation of the spin and charge densities [20-23]. Yet it has not been clear whether static magnetism supports or competes with superconductivity, or if the magnetism and superconductivity coexist in the same microscopic regions of the CuO_2 planes or in different regions. While neutron measurements make it clear that long range magnetic order exists, the Bragg peak intensity integrates over the sample volume and is not, therefore, sensitive to microscopic spatial variations in the order parameter.

Muon spin relaxation (SR) measurements [24,25] provide a complementary probe in this regard. In a magnetic material having a heterogeneous structure, such as "magnetic" and "non-magnetic" regions, SR data are

¹author to whom correspondences should be addressed. E-mail: tom@brentz.phys.columbia.edu

composed of two different signals, corresponding to different environments with signal amplitudes roughly proportional to their volume fractions. Local magnetic fields at muon sites result primarily from the dipolar interaction. In antiferromagnetically ordered systems the local

field decays very quickly with increasing distance from ordered spins, resulting in an effective range of the field of 10–15 Å in cuprate systems. Thus, any heterogeneous magnetic structure in HTSC, having a length scale larger than this, should produce multiple and distinguishable SR signals.

In this paper, we report zero-field (ZF) and transverse-field (TF) SR measurements in a single crystal of $\text{La}_2\text{CuO}_{4.11}$ (LCO :4.11) where excess oxygen is intercalated in a stage-4 structure [16]. This system is superconducting below $T_c = 42$ K. Observation of sharp satellite Bragg peaks in neutron scattering indicates static long range (> 600 Å) spin density wave (SDW) order below $T_N = 42$ K. The modulation wave vector of the SDW is comparable to those observed in $\text{La}_{2-x}\text{Sr}_x\text{CuO}_4$ (LSCO) and $\text{La}_{2-x}\text{Nd}_y\text{Sr}_x\text{CuO}_4$ (LNSCO) systems with the hole concentration $x = 0.125$ [9,12]. The LCO :4.11 system is especially interesting since (a) it has the highest superconducting T_c in the 214 family of materials; (b) it has a rather high magnetic T_N , which is very close to T_c , and well developed long range magnetic order below T_N ; (c) there is no randomness arising from Sr substitution, and the intercalated oxygen ions are three dimensionally ordered. Preliminary results and analysis of our ZF–SR in LCO :4.11 have been presented at a recent conference [26].

We also report SR results in a superconducting $\text{La}_{1.88}\text{Sr}_{0.12}\text{CuO}_4$ (LSCO :0.12) single crystal with $T_c = 30$ K which exhibits magnetic Bragg peaks in neutron scattering [13]. Comparing these results with those of a simulation of the local field distribution at possible muon sites, we examine various models for the magnetically ordered regions. The interplay between superconductivity and magnetism is discussed in the context of the superfluid density $n_s = m$ derived from TF–SR results.

SR studies of magnetism in HTSC systems started in 1987 with studies of antiferromagnetic La_2CuO_4 (AF-LCO) [27], which provided the first evidence of static magnetic order. Subsequently, SR studies on La_2CuO_4 [28], $(\text{La,Li})_2\text{CuO}_4$ [29], $\text{La}_{2-x}\text{Sr}_x\text{CuO}_4$ [30–34], and $\text{YBa}_2\text{Cu}_3\text{O}_{7-y}$ [34,35], were performed to characterize magnetic phase diagrams as a function of hole concentration and also to study details of the spin glass states near $x = 0.05$.

SR measurements of HTSC systems with hole concentration x near $1/8$ were first performed in $\text{La}_{1.875}\text{Ba}_{0.125}\text{CuO}_4$ [36]. These detected static magnetic order below $T_N = 32$ K and a Bessel function

SR line shape, characteristic of spin density wave systems. A reduction of T_c , associated with an increase of the muon spin relaxation due to quasi-static magnetism, was also found by SR in $\text{La}_{2-x}\text{Sr}_x\text{CuO}_4$ near $x = 0.12$ [37]. Recent SR studies on $(\text{La,Nd,Sr})_2\text{CuO}_4$

(LNSCO) [38,39], $(\text{La,Eu,Sr})_2\text{CuO}_4$ (LESCO) [40,41] and $\text{La}_{1.875}\text{Ba}_{0.125-y}\text{Sr}_y\text{CuO}_4$ (LBSCO) [42] found the characteristic Bessel function line shape with the same frequency ~ 3.5 MHz in all these systems. In the latter studies the primary emphasis was determining the magnetic phase diagram as a function of rare-earth and hole concentrations. Although the existence of “zero/low field muon sites”, expected for decomposition of the system into regions with and without static magnetic order, was discussed in these reports [40,42], a systematic study of magnetic volume fraction was not made.

Previously, Pomjakushin et al. [43] reported a SR study for single crystal specimens of $\text{La}_2\text{CuO}_{4+y}$ doped with oxygen, with $y = 0.02$ (LCO :4.02) and 0.04 (LCO :4.04), which have compositions in the miscibility gap between AF-LCO and the stage-6 superconducting compound. In zero field, they observed SR precession signals identical to those found in AF-LCO. With decreasing temperature in LCO :4.02, the amplitude of this oscillatory signal increased from nearly zero above the superconducting $T_c = 15$ K to more than a half of that in AF-LCO at $T = 0$. In LCO :4.04, the oscillatory signal appeared below $T = 230$ K with an amplitude corresponding to approximately a 10% volume fraction for the AF region, and then exhibited a sharp increase below the superconducting $T_c = 25$ K to about a half volume fraction at $T = 0$. In both cases, the amplitudes of the AF oscillation exhibited an increase below T_c . The diamagnetic susceptibility of the LCO :4.02 specimen was, however, destroyed by a small applied field, indicating rather fragile superconductivity. Lack of information about the crystal orientation in the SR measurements prevented a reliable estimate of the volume fraction in this study.

In Section II we present experimental details and results of the ZF–SR measurements. Section III contains our simulation based on a model in which the sample contains microscopic regions where there is full magnetic order and other microscopic regions where the magnetic fields are too small to cause muon precession. In Section IV we present results of measurements in a transverse magnetic field that are sensitive to the superconductivity. Finally in Section V we discuss the results and draw conclusions.

II. ZERO FIELD SR MEASUREMENTS

Single crystals of LCO :4.11 and LSCO :0.12 have been prepared as described in refs. [16] and [13], which report neutron scattering studies of these crystals, respectively. The excess-oxygen doped $\text{La}_2\text{CuO}_{4+y}$ sample is prepared by electrochemically doping a single crystal of pure La_2CuO_4 which is grown by the traveling solvent coating-zone method. The crystal has a mass of 4.21 grams and is cylindrical in shape. As a result of twinning, there are equal populations of two twin domains with either the *a* or *b* crystallographic axis (in orthorhombic no-

tation) nearly parallel to the cylinder's long-axis. In both twin domains, the c-axis is perpendicular to the long-axis. Thermogravimetric analysis on our samples has been performed on two smaller $\text{La}_2\text{CuO}_{4+y}$ crystals with $T_c = 42\text{K}$. We find oxygen concentrations of $y = 0.10(1)$ and $y = 0.12(1)$. The large crystal has the same T_c , so its oxygen concentration is expected to correspond to $y = 0.11(1)$.

Neutron diffraction measurements have shown that this material has a structural modulation along the c-axis corresponding to stage-4. [16]. Further details regarding the characterization of the stage-4 crystal by neutron scattering, susceptibility, and transport techniques may be found in references [16] and [44].

SR measurements were performed at TRIUMF, using a surface muon beam with an incident muon momentum of $28\text{ MeV}/c$, following the standard procedure described in refs. [24,25]. We employed the so-called "low-background" muon spectrometer, which has the capability of vetoing events from muons landing in areas other than the specimen, to ensure much less than 10 % background signal in our SR data. In ZF-SR, we observed positron time spectra via counters placed forward (F) and backward (B) to the incident beam direction (\hat{z}), with the polarization of incident muons \vec{P} antiparallel to \hat{z} . The muon spin relaxation function $G_z(t)$ was obtained from forward (F) and backward (B) time spectra as

$$G_z(t) = [B(t) - F(t)]/[F(t) + B(t)] \quad (1);$$

after correcting for the difference in effective solid angles of the F and B counters. As illustrated in Fig. 1(a), two sets of measurements were made with the c-axis of the specimen mounted parallel (configuration CZ-I) and perpendicular (CZ-II) to \hat{z} .

Figures 2(a) and (b) show the muon spin polarization function $G_z(t)$ observed in these two crystals for CZ-I and CZ-II. Also included are the results obtained for ceramic specimens of non-superconducting $\text{La}_{1.875}\text{Ba}_{0.125}\text{CuO}_4$ (LBCO :0.125) [36] and $\text{La}_{1.475}\text{Nd}_{0.4}\text{Sr}_{0.13}\text{CuO}_4$ (LNSCO :0.13) [38].

We see almost no relaxation above T_N in the time range $t \leq 1\text{ ns}$. Below $T_N = 42\text{ K}$ of LCO :4.11 and $T_N = 20\text{ K}$ of LSCO :0.12, a small oscillatory component appears, with a Bessel-function line shape characteristic of muon precession in SDW systems [45,46]. The amplitude A_{or} of this oscillating and relaxing signal is limited to about 34 % (CZ-I) and 24 % (CZ-II) at $T = 0$ for LCO :4.11, and 20 % (CZ-I) and 10 % (CZ-II) for LSCO :0.12. If we define the internal field at a muon site as \vec{H} and θ is the angle between \hat{z} and \vec{H} , as illustrated in Fig. 1(b), the oscillatory / relaxing amplitude represents $\sin^2(\theta)$ averaged over all the muon sites. In a ceramic specimen which undergoes magnetic order in 100 % of the volume, this amplitude is 67 % ($= 2/3$), as shown in the case of LBCO :0.125. Therefore, the observed signal amplitudes A_{or} for LCO :4.11 and LSCO :0.12 are less

than a half the value expected for a sample with a SDW uniformly established throughout its volume.

In single-crystal specimens, A_{or} can have a small value if the local fields \vec{H} for the majority of muon sites are parallel to \hat{z} . For this case, however, one should see a large A_{or} when the crystal orientation is rotated by 90 degrees from CZ-I to CZ-II or vice versa. Thus, our results, with small A_{or} values for the both configurations, cannot be attributed to such anisotropy. In view of the symmetry of the LCO and LSCO structures, the "powder average" value of $A_{\text{or, powd}}$ can be obtained [26] as

$$A_{\text{or, powd}} = (1/3) [A_{\text{or, CZ-I}} + 2A_{\text{or, CZ-II}}]; \quad (2);$$

which yields 27 % for LCO :4.11 and 12 % for LSCO :0.12. The reduction of $A_{\text{or, powd}}$ from 66.7 % indicates the existence of "zero/low-field" muon sites.

We have analysed the ZF-SR data by fitting the results at $t \leq 1\text{ ns}$ to

$$G_z(t) = A_{\text{or}} j_0(\omega t) \exp(-\lambda t) + A_n \exp[-t^2/\tau^2] \quad (3);$$

where j_0 is the 0-th order Bessel function and A_n represents the non-oscillating amplitude. The first exponential term represents the damping of the Bessel oscillation, whereas the second describes the slow decay due to nuclear dipolar fields. We obtain the volume fraction V of muon sites that experience the SDW field using

$$V = A_{\text{or, powd}}/(2/3); \quad (4)$$

with $A_{\text{or, powd}}$ determined from Eq. (2) at the lowest temperature. We then scale the values for higher temperatures using A_{or} results for the CZ-I configuration. For our t range of $t \leq 1\text{ ns}$, those muon sites with $H \leq 30\text{ G}$ contribute to the first term in Eq. 3, and thus are identified as "nite-field muon sites".

Figures 3(a) and (b) show the temperature dependence of V and the oscillation frequency $\omega = \gamma H = 2\pi/\tau$ for LCO :4.11, LSCO :0.12, LBCO :0.125 [36] and LNSCO :0.13 (ceramic) [38]. The common Bessel-function line shape and the nearly identical frequency

3.5 MHz (corresponding to maximum internal field of 260 G) at $T = 0$ for all the four systems indicate that the spin configurations and magnitudes of the static Cu moments (proportional to $\langle S_z \rangle$) surrounding the "nite-field muon sites" are identical for all the four systems. The volume fraction V increases progressively below T_N with decreasing temperature, in both LCO :4.11 and LSCO :0.12. The frequency acquires its full value just below T_N in LCO :4.11. In Fig. 3(c), we compare the temperature dependence of the neutron Bragg-peak intensity I_B of LCO :4.11 [16] with V^2 from SR. The good agreement of neutron and muon results indicate that these two probes detect the same static magnetism even though the former measures the ordered moment over distances $\sim 600\text{ \AA}$. The SR results suggest that the observed temperature dependence of I_B should be

ascribed mainly to the change of the site fraction containing ordered Cu spins, rather than to the increase of the static moment on individual Cu atoms although this is model dependent.

To illustrate further this unusual temperature dependence of the magnetic order parameter in LCO :4.11, we compare ZF-SR spectra of LCO :4.11 and AF-LCO ($T_N = 250$ K) in Fig. 4. In AF-LCO (Fig. 4(b)), as in most conventional magnetic systems where long-range magnetic order develops in 100 % of the volume, ZF-SR data exhibit muon spin precession whose amplitude is nearly independent of temperature, but whose frequency increases with decreasing temperature. In contrast, for LCO :4.11 (Fig. 4(a)) the oscillation amplitude increases gradually with decreasing temperature below T_N while the frequency just below T_N is already close to the low-temperature value. This implies that in LCO :4.11 the local order is well developed but dynamic above T_N , and the ordering process below T_N involves the ordering of this local magnetism over long distances with a concomitant freezing of the spins.

III. SIMULATION OF ZERO-FIELD SR

To explore the possible origin of the two kinds of muon sites, we have performed computer simulations of the local field distributions at possible muon sites. The location of the muon site in AF-LCO has been approximated by Hitt et al. [47] to be about 1 Å away from the apical oxygen, based on the expected length of the $O^{2-}-H$ hydrogen bond. We have improved their estimate by taking into account the tilt of the CuO_6 octahedra and by comparing the observed SR precession frequency $\omega = 5.8$ MHz with the Cu long-range ordered moment size $0.55 \mu_B$ in AF-LCO [16]. Figure 5 shows the location of the apical-oxygen muon site at (0.199d, 0d, 0.171c) in the unit cell with $d = 3.779$ Å, and $c = 13.2$ Å assumed in this simulation. Since the direction of H is very sensitive to a small change of the tilt angle of the CuO_6 octahedra, we calculate the expected ZF-SR line shape for the powder-average.

Figure 6(a) shows the line shape for this apical-oxygen muon site for: (1) a 100 % volume fraction of antiferromagnetically (AF) ordered Cu moments having modulation vector k_{AF} with ordered moment of $0.55 \mu_B$ (chain-dotted line); and (2) Cu spins with an incommensurate SDW amplitude modulation superimposed on the antiferromagnetic correlations, with a maximum static Cu moment value of $0.35 \mu_B$ (broken line). Here we have assumed that the SDW propagation vector is along the Cu-O-Cu bond direction (i.e., 45 degrees to the orthorhombic a and b axes) with magnitude $k = 2\pi/d = 0.12$ ($d = 3.78$ Å is the distance between nearest neighbour Cu atom s) We have calculated the spin polarization using

$$\cos(k_{AF} \cdot x) = \cos(k \cdot x) =$$

$$(1/2) \cos[(k_{AF} + k) \cdot x] + (1/2) \cos[(k_{AF} - k) \cdot x]; \quad (5)$$

at a given position x . These results confirm that the SDW model gives a line shape nearly identical to a Bessel function (solid line). In AF-LCO the observed SR results [27,47] show a substantial damping of the sinusoidal precession, due to various possible origins, such as nuclear dipolar fields, variations of the muon site or crystal in perfection. To account for the reduction of the observed SR frequency from 5.8 MHz in AF-LCO to 3.64 MHz at $T = 0$ in LCO :4.11, we need to assume that the maximum static Cu moment size in the SDW modulation is $0.36 \mu_B$. This may be compared with the bare Cu moment of $1.1 \mu_B$.

Since there is a substantial density of intercalated oxygen in LCO :4.11, we have also modeled the field distribution at several locations 1 Å away from the expected site of the intercalated oxygen atoms. As may be seen from Fig. 6(b), which displays decay curves calculated for 100 % ordered SDW Cu moments with maximum moment size of $0.35 \mu_B$, there is no muon site location having zero or low internal field. Therefore, we cannot ascribe the existence of "zero/low-field sites" in LCO :4.11 to intercalated oxygen. Furthermore, in LSCO :0.12, there is, of course, no intercalated oxygen, so it seems clear that the non-magnetic sites must have a different origin.

In Fig. 7(a), we show the line shape $G_z(t)$ calculated for Cu moments in circular islands of SDW order in the CuO_2 planes, for various volume fractions V_{Cu} of static Cu spins, assuming the radius R of the circular islands to be $R = 50$ Å. Bessel function line shapes are obtained with a common frequency, while the regions without static Cu moments account for the zero-field sites. The size of the magnetic island is reflected in the damping of the Bessel oscillation.

In Fig. 7(b) we compare the results of simulations for two different geometries. One is for circular magnetic islands with $V_{Cu} = 50\%$ and $R = 15$ and 100 Å. The other corresponds to an "ordered sandwich" model, where two out of every four CuO_2 planes contain completely ordered SDW Cu spins while the other two planes, presumably those adjacent to the intercalated O layers, have no static Cu spins. The curve for $R = 15$ Å islands shows a fast damping of the Bessel oscillation, together with a slow decay of the non-oscillating signal. In contrast, the curves for $R = 100$ Å islands and for the sandwich model exhibit a long-lived Bessel oscillation, with little decay of the non-oscillating signal.

After generating line shapes for the SDW-island model, we have fitted the simulation results to the functional form of Eq. 3. Figure 8(a) shows the resulting magnetic site fraction V as a function of volume fraction containing static Cu spin order V_{Cu} . We see that V increases linearly with increasing Cu fraction, with a slope that is independent of island size R . The site fraction V becomes nearly 100 % at $V_{Cu} = 75\%$. This implies that even the observation of a magnetic SR signal corresponding to $V = 100\%$ cannot rule out the existence

of regions of non-ordered Cu moments in 25 % of the volume. By using the relationship between V and V_{Cu} , we estimate as lower limits $V_{Cu} = 27\%$ for our crystal of LCO :4:11 and 10 % for LSCO :0:12. Of course, this same possible difference between V and V_{Cu} applies in all other copper oxide SDW systems.

In Fig. 8(b), we show the dampening rate of the Bessel function oscillation. We find that a smaller radius R of the island results in a larger γ . We also fit the observed spectra in LCO :4:11 with Eq. 3 and plot the corresponding point in Fig. 8(b) (open star symbol). The result $\gamma_{4:11} = 1.25 \text{ s}^{-1}$ agrees well with the simulation for $R = 15 \text{ \AA}$. In actual systems, however, additional factors cause dampening of the Bessel oscillation, such as variations in the muon site, nuclear dipolar fields, and the effects of imperfections.

To account for these additional effects, we have fit the spectrum of AF-LCO at $T = 20 \text{ K}$ in Fig. 4(b) with the simple form $\cos(\omega t + \phi)$ multiplied by an exponential decay $\exp(-\gamma t)$, and obtain $\gamma_{AF} = 0.81 \text{ s}^{-1}$. Assuming that γ_{AF} represents the additional relaxation contributions, we have obtained a corrected relaxation rate from

$$\gamma_{4:11}^c = (\gamma_{4:11}^2 + \gamma_{AF}^2)^{1/2} \quad (6)$$

That is, we assume that the decay constants add in quadrature.

$\gamma_{4:11}^c$ is shown by the closed star symbol in Fig. 8(b). These considerations lead us to estimate $R = 15 - 30 \text{ \AA}$ for the average radius of the static magnetic islands in LCO :4:11. A similar analysis for LSCO :0:12 would give roughly the same estimate for R . However, because the oscillation amplitude in LSCO :0:12 is much smaller than that in LCO :4:11, the analysis would be less reliable.

It is also possible to obtain the relaxation rate expected for the sandwich model. The result ($\gamma = 0.2 \text{ s}^{-1}$), shown in Fig. 8(b) by the asterisk symbol, indicates that this model is less successful than the magnetic island model in reproducing the relaxation $\gamma_{4:11}$ observed in LCO :4:11.

We now discuss a simple heuristic model for the propagation of magnetic order between these presumed islands. If we assume that spins in neighbouring islands in the same CuO_2 plane are correlated when there is any overlap in the islands' area, as illustrated in Fig. 9, we can estimate the effective correlation length of the spin order. For various values of V_{Cu} we have calculated the probability that the direction of the Cu spins in the magnetic islands, located at a distance r from a Cu spin in the center of a magnetic island, is correlated with the direction of the Cu spin at $r = 0$. The results of this calculation, shown in Fig. 9, suggest that even with the assumption that the spins are in islands, the order in a given plane may nevertheless propagate over long distances. However, for $V_{Cu} = 30\%$ the correlation length from Fig. 9 is only 3 times the size of the magnetic island, whereas the narrow SDW peaks observed in neutron scattering measurements indicate that the static spins are correlated over very large distances ($> 600 \text{ \AA}$) within the plane

[16]. Therefore, some additional mechanism to increase the connectivity is required.

The results in Fig. 9 are obtained assuming no spin correlations between magnetic islands belonging to different neighbouring CuO_2 planes. The neutron measurements of LCO :4:11 [16] indicate that the static SDW order exhibits short range correlations along the c -axis direction with a correlation length of $\sim 13 \text{ \AA}$, somewhat larger than twice the distance between adjacent CuO_2 planes. Such spin correlations along the c -axis direction would further increase the size of the correlated clusters shown in Fig. 9. For example, if we allow correlations when any overlap exists among areas of the islands projected to the adjacent island on neighbouring planes, the effective number of islands contributing to the "connectivity" would increase at least by 3 times compared to the case without interplane correlations. This is because all the islands on a given CuO_2 plane plus those on the upper and lower planes would participate in the correlations.

In Fig. 10, we illustrate this by showing randomly positioned islands of 30 % integrated area fraction in three different planes (a)-(c). When we overlap these planes, almost all the islands achieve percolation, as shown in Fig. 10(d). Moreover, there could be further contribution from islands on the second neighbour planes which would enhance connectivity within the first neighbour planes. In this way, we expect a strong tendency towards percolation of spin correlations among randomly positioned magnetic islands.

IV. SUPERCONDUCTING PROPERTIES

TF-SR measurements allow us to derive the magnetic field penetration depth from the superconducting contribution of the muon spin relaxation rate as $\lambda^2 = \hbar^2 / 4\pi e^2 n_s m$ (superconducting carrier density / effective mass). This rate reflects the inhomogeneity of the magnetic field in the flux vortex structure, which varies over a length scale of $\sim 1000-3000 \text{ \AA}$. Any heterogeneity in the superconducting properties at length scales shorter than this will be averaged out. Thus, SR probes superconductivity with a 100 times coarser spatial resolution than that with which it probes static magnetism. In HTSC systems without any static magnetic order, the line shapes in TF-SR spectra can be used to study more detailed spatial features, such as the size of the vortex core region [48]. In the present case, with co-existing superconductivity and static magnetic order, however, detailed line-shape analyses become very difficult.

We have performed TF-SR measurements by rotating the incident muon polarization to be perpendicular to the beam $\vec{P} \perp \hat{z}$ and applying an external field parallel to \hat{z} with the c -axis of the specimen mounted either parallel to \hat{z} [configuration CT-I] or perpendicular to \hat{z} [con-

ration CT-II], as illustrated in Fig. 11. The muon spin polarization function $G_x(t)$ is measured using two sets of counters placed up (U) and down (D) of the incident beam.

As shown in Figs. 12 (a) and (b), we observe a larger relaxation in CT-I, the geometry reflecting the in-plane penetration depth λ_{ab} , than in CT-II. We have analyzed the TF-SR results by assuming the existence of a static internal field in a volume fraction V of muon sites, having the distribution in magnitude and direction estimated from the ZF-SR measurements. We have then added vectorially the external field, with a Gaussian broadening due to superconductivity. For the "zero/low-field muon sites" with volume fraction $(1-V)$, we assume that the muon sees only the nuclear dipolar fields and the Gaussian-broadened external field. We fit the observed data with this model, and derive the Gaussian halfwidth at half maximum of the superconducting contribution equal to λ_{ab} . Figure 12 (a) shows the calculated contributions to the relaxation from superconductivity and static magnetism, separately.

The temperature dependence of λ_{ab} , observed in the CT-I configuration, is shown in Fig. 13 for LCO :4.11 and LSCO :0.12. The relaxation rate shows a gradual increase with decreasing temperature below T_c . To compare the values of $\lambda_{ab}(T \rightarrow 0)$ with those observed in ceramic specimens of other HTSC systems [49-52], we multiply by 1/1.4 to account for the effect of the anisotropic penetration depth [53]. We then add the corresponding points to the plot of $\lambda_{ab}(T \rightarrow 0)$ versus T_c in Fig. 14. The points for the present systems lie on the same trajectory as other LSCO systems. We have also included a point for LESCO (Eu0.1, Sr0.15; ceramic), which exhibits static magnetic order with $V = 50\%$ [40,54,55]. This point again falls on the trajectory. The correlation in Fig. 14 suggests that λ_{ab} / n_s at $T \rightarrow 0$ is a determining factor for T_c in HTSC systems with static stripe freezing (present systems and LESCO) in a way similar to the case for underdoped [49,50], Zn-doped [52] and overdoped [51,56] HTSC systems.

V. DISCUSSION AND CONCLUSIONS

A. Interplay between magnetic and superconducting volumes

Comparing the results of λ_{ab} to those observed in ceramic LSCO systems, assuming that λ_{ab} is independent of doping, the results for LCO :4.11 and LSCO :0.12 correspond to volume average hole densities of 0.14 ± 0.02 and 0.10 ± 0.02 holes per Cu, respectively. In view of the large systematic errors, however, we can not use these results to distinguish whether the volume without static magnetism $(1-V_{Cu})$ alone or the total volume carries superconductivity. We can rule out, however, a case where superconducting carriers exist only in the mag-

netic volume V_{Cu} , since the local hole-concentration for this model would need to be unrealistically large (more than 0.3 holes per Cu) to account for the observed value of volume integrated n_s , which is comparable to those in LSCO systems in the optimum-doping region. So far, a clear indication of mutually exclusive regions with static magnetism and superconductivity has been obtained only in SR measurements in $(La, Eu, Sr)_2CuO_4$ (LESCO) [40,54,55], which demonstrate that the superfluid density n_s scales as $(1-V)$.

In previous work on $La_{1.45}Nd_{0.4}Sr_{0.15}CuO_4$ and $La_{1.45}Nd_{0.4}Sr_{0.2}CuO_4$ [38], which are superconducting below $T_c = 7$ K and 12 K, respectively, $V = 100\%$ was found. This result could be interpreted as evidence of spatial overlap of regions supporting superconductivity and regions having static spin order. The relationship in Fig. 8 (a), however, indicates that V_{Cu} for this system can be smaller than 100%. This leaves open the possibility that superconductivity with reduced T_c survives in a small remaining volume fraction $(1-V_{Cu}) = 20\%$, while superconducting regions and regions with static magnetism are mutually exclusive.

The situation with magnetic islands, having length scales comparable to the in-plane superconducting coherence length, resembles the "swiss cheese model" [52] for Zn-doped HTSC systems, where a non-superconducting region of comparable size is created around each Zn. This model was proposed based on the SR results for the reduction of n_s as a function of Zn concentration [52], and was recently confirmed by direct measurements of scanning tunnelling microscopy (STM) [57]. The SR results for overdoped HTSC systems can also be explained if one assumes spontaneous formation of hole-rich non-superconducting islands embedded into a sea of hole-poor superfluid [55, 58-60]. The correlation between T_c and n_s survives in all these systems, as shown in Fig. 14. We note that similar microscopic heterogeneity in the superconducting state has also been found in recent STM measurements on underdoped Bi2212 systems [61].

The T_c vs. n_s correlations are robust against various perturbations in HTSC materials, such as those caused by Zn-in-purities, overdoped fermion carriers, and the formation of static magnetic islands, seen in the present work. This is analogous to the robustness of correlations between the superfluid transition temperature and the 2-dimensional superfluid density in thin films of 4He and $^3He/^4He$ adsorbed in porous and non-porous media [62-66]. Based on these observations, one of us [55,59,60] pointed out a possible relevance of these heterogeneous electronic/magnetic features in HTSC systems to a "microscopic phase separation", such as the one seen in superfluid $^3He/^4He$ films adsorbed in porous media / fine powders [66,67].

In the present work on LCO :4.11, as well as a previous SR study on LCO :4.02 and LCO 4.04 [43], the onset of superconductivity occurs around the temperature below which the volume fraction of static magnetism increases with decreasing temperature. This apparent coincidence

of T_c and T_N could be expected if a microscopic rearrangement of charge distribution occurs at T_c . T_N to separate the electron systems into hole-rich regions which support superconductivity and hole-poor ($x = 1/8$ for LCO :4.11 and $x = 0$ for LCO :4.02 and LCO :4.04) regions which support static magnetism.

Recently, Kivelson et al. [68] have proposed a model with a particular type of phase separation to explain the sharp rise of χ and gradual increase of V_{Cu} below T_N seen in the present study of LCO :4.11. Their model also predicts a trade-off of superconducting and magnetic volumes below T_c . The gradual change of both $\chi(T)$ and $V(T)$ below T_c in LCO :4.11 (Figs. 3(a) and 13), however, seems inconsistent with such a trade-off.

The superconducting T_c and the magnetic T_N appear at different temperatures in SR measurements of LSCO :0.12 as well as in various LN SCO and LESCO systems, with LSCO :0.12 having $T_c > T_N$ and the other materials having $T_N > T_c$. It should be noted that neutron measurements give $T_c' < T_N$ in LSCO :0.12, while T_N determined by SR is lower, presumably due to difference in time windows between neutron and muon measurements. In these systems the frequency increases with decreasing temperature gradually below T_N , as shown in Fig. 3(b), and in refs. [38-42]. Thus, the abrupt development of the magnetic order parameter is not a common feature of all the HTSC systems.

B. Bragg peak intensity in LCO :4.11 and AF-LCO

We can estimate the Bragg peak intensity $I_{B:4.11}$ expected in neutron scattering measurements on LCO :4.11 from the SR results. $I_{B:4.11}$ should be reduced from the value $I_{B:AF}$ in AF-LCO by a factor 0.5 for the SDW amplitude (\sin^2) times the ratio of the maximum static moments $(0.36/0.55)^2$ times the volume fraction of magnetic Cu atoms $V_{Cu} = 0.27$. Thus, we predict as a rough estimate $I_{B:4.11} = 0.06 I_{B:AF}$. This value agrees well with the observed neutron results $I_{B:4.11} = 0.07 I_{B:AF}$. In Reference [16] it is assumed that three out of four copper ions are magnetic and that they are distributed uniformly throughout the entire volume, so a smaller average moment per Cu^{2+} of 0.15 μ_B is inferred.

We note, however, that estimates of the ordered moment size from neutron studies and from SR often disagree with one another. For example, the Néel temperature in antiferromagnetic La_2CuO_{4+x} varies from $T_N = 300$ K to $T_N = 100$ K with a small variation in x . In neutron scattering studies of these AF-LCO systems, the Bragg peak intensity I_B shows a reduction, by more than a factor of 10, with decreasing T_N [28]. In contrast, the frequency of ZF-SR spectra shows only a 20 % change in the local frozen moment for the same reduction of T_N . These SR and neutron results on AF-LCO are compared in ref. [28]. Since the SR frequency is directly proportional to the magnitude of neighbouring

static Cu moments, the reduction of I_B in neutron studies cannot be ascribed to a change of individual Cu moment size. The likely reason for the strong reduction of I_B is a progressive trade-off between the true long range ordered component and short range spin glass fluctuations which recent work [69] has shown involves fluctuations into the diagonal stripe spin glass phase with hole concentration of 0.02.

C. Neutron results in high magnetic fields

Recently Khaykovich et al. [48] have made measurements on LCO :4.11 in high magnetic fields H_{ext} applied parallel to the c-axis. By increasing the external field from $H_{ext} = 0$ to $H_{ext} = 9$ T, they have found a factor 2 increase of the intensity I_B of the magnetic Bragg peak at $T = 0$ for a crystal similar to the one studied here. The superconducting T_c is suppressed by H_{ext} , while T_N remains nearly unchanged up to $H_{ext} = 9$ T.

Application of H_{ext} perpendicular to the CuO_2 plane creates vortices. The vortex core, with radius comparable to the in-plane coherence length $\xi_{ab} = 30$ Å becomes normal, as illustrated in Fig. 15. These normal cores could have static magnetic order similar to that in the surrounding magnetic islands.

The fraction of the area contained in vortex cores may be estimated from the upper critical field, since that is the field at which the cores fill the entire area. Using $H_{c2} = 40$ T, found for optimally doped LSCO [70], we expect that only $1/4$ or less of the area that is superconducting at $H_{ext} = 0$ would be turned into a normal core at $H_{ext} = 9$ T. However, this is sufficient to explain the factor 2 increase in the Bragg peak intensity if the zero-field sample has ordered moments in only 27% of its volume and if the magnetism in the cores is coherent with the long range order present at zero field. We are currently undertaking SR studies of LCO :4.11 in high applied magnetic fields, which will be reported in future publications.

In nearly optimally doped LSCO, Lake et al. [71] have recently found that low-energy neutron scattering intensity, below the energy transfer corresponding to the superconducting energy gap, increases at temperatures well below T_c , when a high external field H_{ext} is applied along the c-axis. This phenomenon may also be related to the magnetic response from the flux-core regions, since the increase of the intensity sets in at the flux-depinning temperature. A rather surprising feature of this study is the sharpness of the observed low-energy fluctuations in momentum space, suggesting long-range spin correlations among widely separated vortex core regions. We point out here that, like the static order, this requires long range coupling between vortex cores.

In summary, we have performed ZF-SR measurements using LCO 4.11 and LSCO 0.12 single crystals, and have found that static incommensurate SDW spin freezing, with the maximum ordered Cu moment size of $0.36 \mu_B$, develops only in a partial site fraction. We assume $\sim 40\%$ for LCO 4.11 and $\sim 18\%$ for LSCO 0.12, and specimen modeling suggests that the corresponding ordered Cu fractions may be somewhat smaller. Comparison of observed results with computer simulation suggests the formation of static magnetic islands on the CuO_2 planes having size $R = 15 - 30 \text{ \AA}$, comparable to the in-plane superconducting coherence length ξ_{ab} . Order between these islands nevertheless propagates over long distances to yield a correlation length in excess of 600 \AA .

We stress that LCO 4.11, which is a stoichiometric single crystal, has the least built-in randomness among the various HTSC systems that exhibit static incommensurate magnetic correlations. Yet the present work demonstrates that the ground state is a mixture of magnetically ordered and at best weakly ordered regions. Near phase boundaries or quantum critical points in strongly correlated electron systems, such microscopic heterogeneity could result from competition of the different order parameters involved. Related phenomena have been observed, for example, in the formation of stripe magnetic correlations in manganites [72] and the development of stripe domains in LSCO with $x = 0.01$ to 0.02 [73]. These observations encourage further theoretical studies of electronic states involving spontaneous formation of heterogeneous regions in competing order parameter systems.

Our TF-SR measurements in these systems demonstrate that $n_s = m$ at $T \rightarrow 0$ exhibits correlations with T_c not only in underdoped, Zn-doped, and overdoped HTSC systems but also in the present system with static SDW spin freezing. Recent measurements of the penetration depth in $(\text{BEDT-TTF})_2\text{Cu}(\text{NCS})_2$ in applied pressure [74], and in A_3C_{60} systems [75,76], suggest that these correlations are followed also by organic and fullerene superconductors.

We have proposed a model for explaining the rather long-range spin correlations in these systems, resorting to "connectivity" of neighbouring magnetic islands on the same and adjacent CuO_2 planes. We have also suggested that static magnetism in the vortex core region can provide explanations for the field dependence of the neutron scattering results in LCO 4.11 and in optimally doped LSCO systems.

The present work demonstrates a very important feature of SR, i.e., the capability to determine the volume fraction of magnetically ordered regions. Recently, a similar case was noticed in the study of URu_2Si_2 , where static magnetism below $T_N = 17 \text{ K}$ has been identified to exist in a partial volume fraction by combination

of neutron [77] and NMR [78] studies in applied pressure. The first evidence for this feature was indeed provided by a SR measurement [79] in ambient pressure. In the SR results for URu_2Si_2 , Luke et al. found a very sharp onset of the precession frequency $\omega(T)$ below T_N , temperature dependence of the precession amplitude $V(T)$, and a good agreement between the temperature dependence $I_B(T)$ of the neutron Bragg peak and V^2 from SR. These features are common to the present results in LCO 4.11. We also note that ZF-SR results in $\text{CeCu}_{2.2}\text{Si}_2$ [80,81] indicate a possible trade-off between magnetic and superconducting volume fractions. These results suggest possible involvement of microscopic phase separation in both HTSC systems and heavy fermion systems [55,68,82]. Further detailed studies of SR in combination with neutron scattering will be very helpful in obtaining an overall understanding of the interplay between magnetism and superconductivity in HTSC, heavy-fermion, and other strongly correlated electron systems.

VI. ACKNOWLEDGEMENT

We wish to acknowledge helpful discussions with B. Nachum, G. Shirane, J.M. Tranquada and S. Uchida. The work at Columbia was supported by NSF (DMR-98-02000 and DMR-01-02752) and US-Israel Binational Science Foundation. Research at McMaster is supported by NSERC and the Canadian Institute for Advanced Research. The work at MIT has been supported by the MRSEC Program of the National Science Foundation under Award No. DMR 9808941 and by NSF under Awards No. DMR 0071256 and DMR 99-71264. Work at the University of Toronto is part of the Canadian Institute for Advanced Research and is supported by the Natural Science and Engineering Research Council of Canada.

-
- [1] For general review of magnetic and superconducting properties of HTSC systems, see, for example, M.A. Kastner, R.J. Birgeneau, G. Shirane, and Y. Endoh, Magnetic, transport, and optical properties of monolayer copper oxides, *Rev. Mod. Phys.* 70 (1988) 897.
 - [2] R.J. Birgeneau, Y. Endoh, K. Kakurai, Y. Hidaka, T. Murakami, M.A. Kastner, T.R. Thurston, G. Shirane, and K. Yamada, Static and dynamic spin fluctuations in superconducting $\text{La}_{2-x}\text{Sr}_x\text{CuO}_4$, *Phys. Rev. B* 39 (1989) 2868.
 - [3] Y. Endoh, K. Yamada, R.J. Birgeneau, D.R. Gabbe, H.P. Jenssen, M.A. Kastner, C.J. Peters, P.J. Picon, T.R. Thurston, J.M. Tranquada, G. Shirane, Y. Hidaka, M. Oda, Y. Enomoto, M. Suzuki, T. Murakami, Static and

- dynam ic spin correlations in pure and doped La_2CuO_4 , Phys. Rev. B 37 (1988) 7443.
- [4] G. Shirane, R. J. Birgeneau, Y. Endoh, P. Gehring, M. A. Kastner, K. Kitazawa, H. Kojima, I. Tanaka, T. R. Thurston, K. Yamada, Temperature Dependence of the Magnetic Excitations in $\text{La}_{1.85}\text{Sr}_{0.15}\text{CuO}_4$ ($T_c = 33\text{ K}$), Phys. Rev. Lett. 63 (1989) 330.
- [5] G. Aeppli, T. E. Mason, S. M. Hayden, H. A. Mook, J. Kulkda, Nearly Singular Magnetic Fluctuations in the Normal State of a High- T_c Cuprate Superconductor, Science 278 (1997) 1432.
- [6] H. A. Mook, P. Dai, K. Salama, D. Lee, F. Dogan, G. Aeppli, A. T. Boothroyd, M. E. Mostoller, Incommensurate One-Dimensional Fluctuations in $\text{YBa}_2\text{Cu}_3\text{O}_{6.93}$, Phys. Rev. Lett. 77 (1996) 370.
- [7] H. A. Mook, P. Dai, S. M. Hayden, G. Aeppli, T. G. Perring, F. Dogan, Spin Fluctuations in $\text{YBa}_2\text{Cu}_3\text{O}_{6.6}$, Nature 395 (1998) 580.
- [8] M. Arai, T. Nishijima, Y. Endoh, T. Egami, S. Tajima, K. Tomimoto, Y. Shihara, M. Takahashi, A. Garrett, S. M. Bennington, Incommensurate Spin Dynamics of Underdoped Superconductor $\text{YBa}_2\text{Cu}_3\text{O}_{6.7}$, Phys. Rev. Lett. 83 (1999) 608.
- [9] J. M. Tranquada, B. J. Sternlieb, J. D. Axe, Y. Nakamura, S. Uchida, Evidence for Stripe Correlations of Spins and Holes in Copper Oxide Superconductors, Nature 375 (1995) 561.
- [10] J. M. Tranquada, J. D. Axe, N. Ichikawa, Y. Nakamura, S. Uchida, B. Nachumi, Neutron-scattering study of stripe-phase order of holes and spins in $\text{La}_{1.48}\text{Nd}_{0.4}\text{Sr}_{0.12}\text{CuO}_4$, Phys. Rev. B 54 (1996) 7489.
- [11] J. M. Tranquada, N. Ichikawa, S. Uchida, Glassy Nature of Stripe Ordering in $\text{La}_{1.6-x}\text{Nd}_{0.4}\text{Sr}_x\text{CuO}_4$, Phys. Rev. B 59 (1999) 14712.
- [12] K. Yamada, C. H. Lee, K. Kurahashi, J. Wada, S. Wakimoto, S. Ueki, H. Kimura, Y. Endoh, S. Hosoya, G. Shirane, R. J. Birgeneau, M. G. Reven, M. A. Kastner, Y. J. Kim, Doping Dependence of the Spatially Modulated Dynamical Spin Correlations and the Superconducting-transition Temperature in $\text{La}_2-x\text{Sr}_x\text{CuO}_4$, Phys. Rev. B 57 (1998) 6165.
- [13] T. Suzuki, T. Goto, K. Chiba, T. Shinoda, T. Fukase, H. Kimura, K. Yamada, M. Ohashi, Y. Yamaguchi, Observation of Modulated Magnetic Long-range Order in $\text{La}_{1.88}\text{Sr}_{0.12}\text{CuO}_4$, Phys. Rev. B 57 (1998) R3229.
- [14] S. Wakimoto, R. J. Birgeneau, Y. S. Lee and G. Shirane, Hole concentration dependence of the magnetic moment in superconducting and insulating $\text{La}_2-x\text{Sr}_x\text{CuO}_4$, Phys. Rev. B 63 (2001) 172501.
- [15] B. O. Wells, Y. S. Lee, M. A. Kastner, R. J. Christianson, R. J. Birgeneau, K. Yamada, Y. Endoh, G. Shirane, Incommensurate Spin Fluctuations in High-Transition Temperature Superconductors, Science 277 (1997) 1067.
- [16] Y. S. Lee, R. J. Birgeneau, M. A. Kastner, Y. Endoh, S. Wakimoto, K. Yamada, R. W. Erwin, S. H. Lee, G. Shirane, Neutron-scattering Study of Spin-density Wave Order in the Superconducting State of Excess Oxygen-doped $\text{La}_2\text{CuO}_{4+y}$, Phys. Rev. B 60 (1999) 3643.
- [17] A. Bianconi, A. C. Castellano, M. Desantis, P. Delogu, A. Gargano, R. Giorgi, Localization of Cu-3d levels in the high- T_c superconductor $\text{YBa}_2\text{Cu}_3\text{O}_7$ by Cu-2p X-ray photoelectron spectroscopy, Solid State Commun. 63 (1987) 1009.
- [18] A. Bianconi, The Instability Close to the 2D Generalized Wigner Polaron Crystal Density: A Possible Pairing Mechanism Indicated by a Key Experiment, Physica C 235-240 (1994) 269.
- [19] A. Bianconi, N. L. Saini, T. Rossetti, A. Lanzara, A. Perali, M. Messori, H. Oyanagi, H. Yamaguchi, Y. Nishihara, D. H. Ha, Stripe structure in the CuO_2 plane of perovskite superconductors, Phys. Rev. B 54 (1996) 12018.
- [20] J. Zaanen and O. Gunnarsson, Charged magnetic domain lines and the magnetism of high- T_c oxides, Phys. Rev. B 40 (1989) 7391.
- [21] D. Poilblanc and T. M. Rice, Charged solitons in the Hartree-Fock approximation to the large- U Hubbard model, Phys. Rev. B 39 (1989) 9749.
- [22] V. J. Emery, S. A. Kivelson and H. Q. Lin, Phase separation in the t - J model, Phys. Rev. Lett. 64 (1990) 475.
- [23] V. J. Emery, S. A. Kivelson, O. Zachar, Spin-gap proximity effect mechanism of high-temperature superconductivity, Phys. Rev. B 56 (1997) 6120.
- [24] For a general review of SR, see, for example, A. Schenck, Muon Spin Rotation Spectroscopy, Adam Hilger, Bristol, 1985.
- [25] For a recent reviews of SR studies in topical subjects, see Muon Science: Muons in Physics, Chemistry and Materials, Proceedings of the Fifty First Scottish Universities Summer School in Physics, St. Andrews, August, 1988, ed. by S. L. Lee, S. H. Kilcoyne, and R. Cywinski, Inst. of Physics Publishing, Bristol, 1999.
- [26] A. T. Savici, Y. Fudamoto, I. M. Gat, M. J. Larkin, Y. J. Uemura, K. M. Kojima, Y. S. Lee, M. A. Kastner, R. J. Birgeneau, Static Magnetism in Superconducting Stage-4 $\text{La}_2\text{CuO}_{4+y}$, Physica B 289-290 (2000) 338.
- [27] Y. J. Uemura, W. J. Kossler, X. H. Yu, J. R. Kempton, H. E. Schone, D. Opie, C. E. Stronach, D. C. Johnston, M. S. Alvarez, D. P. Goshom, Antiferromagnetism of $\text{La}_2\text{CuO}_{4+y}$ Studied by Muon Spin Rotation, Phys. Rev. Lett. 59 (1987) 1045.
- [28] Y. J. Uemura, W. J. Kossler, J. R. Kempton, X. H. Yu, H. E. Schone, D. Opie, C. E. Stronach, J. H. Brewer, R. F. Kie, S. R. Kretzmann, G. M. Luke, T. M. Rie-eman, D. L. Williams, E. J. Ansaldo, Y. Endoh, Y. Kudo, K. Yamada, D. C. Johnston, M. S. Alvarez, D. P. Goshom, Y. Hidaka, M. Oda, Y. Enomoto, M. Suzuki, T. Murakami, Comparison between Muon Spin Rotation and Neutron Scattering Studies on the 3-dimensional Magnetic Order of $\text{La}_2\text{CuO}_{4+y}$, Physica C 153-155 (1988) 769.
- [29] L. P. Le, R. H. Heener, D. E. MacLaughlin, K. Kojima, G. M. Luke, B. Nachumi, Y. J. Uemura, J. L. Sarrao, Z. Fisk, Magnetic Behavior in Li-doped La_2CuO_4 , Phys. Rev. B 54, (1996) 9538.
- [30] D. R. Harshman, G. Aeppli, G. P. Espinosa, A. S. Cooper, J. P. Remeika, E. J. Ansaldo, T. M. Rie-eman, D. L. Williams, D. R. Noakes, B. Elman, T. F. Rosenbaum, Freezing of Spin and Charge in $\text{La}_2-x\text{Sr}_x\text{CuO}_4$, Phys. Rev. B 38 (1988) 852.
- [31] B. J. Sternlieb, G. M. Luke, Y. J. Uemura, T. M. Rie-eman,

- J.H. Brewer, P.M. Gehring, K. Yamada, Y. Hidaka, T. Murakami, T.R. Thurston, R.J. Birgeneau, Muon Spin Relaxation and Neutron Scattering Studies of Magnetism in Single-crystal $\text{La}_{1.94}\text{Sr}_{0.06}\text{CuO}_4$, *Phys. Rev. B* 41 (1990) 8866.
- [32] A. Weidinger, Ch. Niedermayer, A. Golnik, R. Simon, E. Recknagel, J.I. Budnick, B. Chamberland, C. Baines, Observation of Magnetic Ordering in Superconducting $\text{La}_{2-x}\text{Sr}_x\text{CuO}_4$ by Muon Spin Rotation, *Phys. Rev. Lett.* 62 (1989) 102.
- [33] F. Borsa, P. Carretta, J.H. Cho, F.C. Chou, Q. Hu, D.C. Johnston, A. Lascialfari, D.R. Torgeson, R.J. Gooding, N.M. Salem, K.J.E. Vos, Staggered Magnetization in ^{139}La NQR and μ -SR, *Phys. Rev. B* 52 (1995) 7334.
- [34] Ch. Niedermayer, C. Bernhard, T. Blasius, A. Golnik, A. Moodenbaugh, J.I. Budnick, Common Phase Diagram for Antiferromagnetism in $\text{La}_{2-x}\text{Sr}_x\text{CuO}_4$ and $\text{Y}_{1-x}\text{Ca}_x\text{Ba}_2\text{Cu}_3\text{O}_6$ as Seen by Muon Spin Rotation, *Phys. Rev. Lett.* 80 (1998) 3843.
- [35] J.H. Brewer, E.J. Ansaldo, J.F. Carolan, A.C.D. Chaklader, W.N. Hardy, D.R. Harshman, M.E. Hayden, M. Ishikawa, N. Kaplan, R. Kettel, J. Kempton, R.F. Kiehl, W.J. Kossler, S.R. Kreitzman, A. Kulp, Y. Kuno, G.M. Luke, H. Miyatake, K. Nagamine, Y. Nakazawa, N. Nishida, K. Nishiyama, S. Ohkuma, T.M. Riseman, G. Roehmer, P. Schleger, D. Shimada, C.E. Stronach, T. Takabatake, Y.J. Uemura, Y. Watanabe, D.L. Williams, T. Yamazaki, B. Yang, Antiferromagnetism and Superconductivity in Oxygen-Deficient $\text{YBa}_2\text{Cu}_3\text{O}_x$, *Phys. Rev. Lett.* 60 (1988) 1073.
- [36] G.M. Luke, L.P. Le, B.J. Sternlieb, W.D. Wu, Y.J. Uemura, J.H. Brewer, T.M. Riseman, S. Isibashi, S. Uchida, Static Magnetic Order in $\text{La}_{1.875}\text{Ba}_{0.125}\text{CuO}_4$, *Physica C* 185-189 (1991) 1175.
- [37] K. Kumagai, K. Kawano, I. Watanabe, K. Nishiyama, and K. Nagamine, SR and NMR investigations on electronic and magnetic state around $x = 0.12$ in $\text{La}_{2-x}\text{Sr}_x\text{CuO}_4$ and $\text{La}_{2-x}\text{Ba}_x\text{CuO}_4$, *Hyperne Interact.* 86 (1994) 473.
- [38] B. Nachumi, Y. Fudamoto, A. Keren, K.M. Kojima, M. Larkin, G.M. Luke, J. Merrin, O. Tchernyshyov, Y.J. Uemura, N. Ichikawa, M. Goto, H. Takagi, S. Uchida, M.K. Crawford, E.M. McCarron, D.E. MacLaughlin, R.H. Heiner, Muon Spin Relaxation Study of the Stripe Phase Order in $\text{La}_{1.6-x}\text{Nd}_{0.4}\text{Sr}_x\text{Cu}_2\text{O}_4$ and Related 214 Cuprates *Phys. Rev. B* 58 (1998) 8760.
- [39] W. Wagener, H.H. Klauss, M. Hillberg, M.A.C. de Melo, M. Birke, F.J. Litterst, E. Schreier, B. Buchner, H. Micklitz, μ -SR in $(\text{La}_{1.85-x}\text{Nd}_x)\text{Sr}_{0.15}\text{CuO}_4$, *Hyperne Interact.* 105 (1997) 107.
- [40] K.M. Kojima, H. Eisaki, S. Uchida, Y. Fudamoto, I.M. Gat, A. Kinkhabwala, M.I. Larkin, G.M. Luke, Y.J. Uemura, Magnetism and Superconductivity of High- T_c Cuprates $(\text{La},\text{Eu},\text{Sr})_2\text{CuO}_4$, *Physica B* 289 (2000) 373.
- [41] H.H. Klauss, W. Wagener, M. Hillberg, W. Kopmann, H. Wolf, F.J. Litterst, M. Hucker, B. Buchner, From Antiferromagnetic Order to Static Magnetic Stripes: The Phase Diagram of $(\text{La},\text{Eu})_2\text{Sr}_x\text{CuO}_4$, *Phys. Rev. Lett.* 85 (2000) 4590.
- [42] A. Lappas, K. Prassides, F.N. Gygax, A. Schenck, Magnetic and Structural Instabilities in the Stripe-phase Region of $\text{La}_{1.875}\text{Ba}_{0.125-y}\text{Sr}_y\text{CuO}_4$ ($0 \leq y \leq 0.1$), *J. Phys. Cond-Mat* 12 (2000) 3401.
- [43] V. Yu. Pomjakushin, A.A. Zakharov, A.M. Balagurov, F.N. Gygax, A. Schenck, A. Amato, D. Herlach, A.J. Beskrovny, V.N. Duginov, Yu.V. Oboukhov, A.N. Ponomarev, S.N. Barilo, Microscopic Phase Separation in $\text{La}_2\text{CuO}_{4+y}$ Induced by the Superconducting Transition, *Phys. Rev. B* 58 (1998) 12350.
- [44] B. Khaykovich, Y.S. Lee, S. Wakimoto, K.J. Thomas, R. Erwin, S.-H. Lee, M.A. Kastner, R.J. Birgeneau, Enhancement of Long-Range Magnetic Order by magnetic field in superconducting LaCuO_4 , *cond-mat/0112505*.
- [45] L.P. Le, A. Keren, G.M. Luke, B.J. Sternlieb, W.D. Wu, Y.J. Uemura, J.H. Brewer, T.M. Riseman, R.V. Upasani, L.Y. Chiang, W. Kang, P.M. Chaikin, T. Csiba, G. Grunner, Muon Spin Rotation/Relaxation Studies in $(\text{TM T SF})_2\text{-X}$ Compounds, *Phys. Rev. B* 48 (1993) 7284.
- [46] L.P. Le, R.H. Heiner, J.D. Thompson, G.J. Nieuwenhuys, D.E. MacLaughlin, P.C. Canfield, B.K. Chyo, A. Amato, R. Feyerherm, F.N. Gygax, A. Schenck, SR studies of borocarbides, *Hyperne Interact.* 104 (1997) 49.
- [47] B. Hitti, P. Birrer, K. Fischer, F.N. Gygax, E. Lippelt, H.M. Aletta, A. Schenck, M. Welter, Study of La_2CuO_4 and related compounds by SR, *Hyperne Interact.* 63 (1990) 287.
- [48] J.E. Sonier, J.H. Brewer, R.F. Kiehl, SR Studies of the Vortex State in Type-II Superconductors, *Rev. Mod. Phys.* 72 (2002) 769.
- [49] Y.J. Uemura, G.M. Luke, B.J. Sternlieb, J.H. Brewer, J.F. Carolan, W.N. Hardy, R. Kadono, J.R. Kempton, R.F. Kiehl, S.R. Kreitzman, P.M. Ulhem, T.M. Riseman, D.L. Williams, B.X. Yang, S. Uchida, H. Takagi, J. Gopalakrishnan, A.W. Sleight, M.A. Subramanian, C.L. Chien, M.Z. Cieplak, Gang Xiao, V.Y. Lee, B.W. Statt, C.E. Stronach, W.J. Kossler, and X.H. Yu, Universal Correlations between T_c and n_s/m (Carrier Density over Effective Mass) in High- T_c Cuprate Superconductors, *Phys. Rev. Lett.* 62, (1989) 2317.
- [50] Y.J. Uemura, L.P. Le, G.M. Luke, B.J. Sternlieb, W.D. Wu, J.H. Brewer, T.M. Riseman, C.L. Seaman, M.B. Maple, M. Ishikawa, D.G. Hinks, J.D. Jorgensen, G. Saito, and H. Yamochi, Basic Similarities among Cuprate, Bismuthate, Organic, Chevrel-Phase and Heavy-Fermion Superconductors Shown by Penetration-Depth Measurements, *Phys. Rev. Lett.* 66, (1991) 2665.
- [51] Y.J. Uemura, A. Keren, L.P. Le, G.M. Luke, W.D. Wu, Y. Kubo, T. Manako, Y. Shimakawa, M. Subramanian, J.L. Cobb, and J.T. Markert, Magnetic Field Penetration Depth in $\text{Tl}_2\text{Ba}_2\text{CuO}_{6+x}$ in the Overdoped Regime, *Nature (London)* 364 (1993) 605.
- [52] B. Nachumi, A. Keren, K. Kojima, M. Larkin, G.M. Luke, J. Merrin, O. Tchernyshov, Y.J. Uemura, N. Ichikawa, M. Goto, and S. Uchida, Muon Spin Relaxation Studies of Zn-Substitution Effects in High- T_c Cuprate Superconductors, *Phys. Rev. Lett.* 77, (1996) 5421.
- [53] W. Barford and J.M.F. Gunn, The theory of the mea-

- measurements of the London penetration depth in uniaxial type-II superconductors by muon spin rotation, *Physica C* 156 (1988) 515.
- [54] K.M. Kojima, T. Kakeshita, T. Ono, H. Eisaki, S. Uchida, Y. Fudamoto, I. Gat, M.J. Larkin, G.M. Luke, Y.J. Uemura, SR Evidence for Coexisting Spin Stripe and Superconductivity Order in $\text{La}_{2-x}\text{Eu}_y\text{Sr}_x\text{CuO}_4$, unpublished.
- [55] Y.J. Uemura, Superfluid Density, Condensation, and Phase Separation in High- T_c and Other Exotic Superconductors, *Physica C* 341-348 (2000) 2117.
- [56] Ch. Niedermayer, C. Bernhard, U. Binniger, H. Gluckler, J.L. Tallon, E.J. Ansaldo, and J.I. Budnick, Muon Spin Rotation Study of the Correlation Between T_c and n_s in Overdoped $\text{TlBa}_2\text{CuO}_{6+x}$, *Phys. Rev. Lett.* 71 (1993) 1764.
- [57] S.H. Pan, E.W. Hudson, K.M. Lang, H. Eisaki, S. Uchida, J.C. Davis, Imaging the Effects of Individual Zinc Impurity Atoms on Superconductivity in $\text{Bi}_2\text{Sr}_2\text{CaCu}_2\text{O}_{8+x}$, *Nature (London)* 403 (2000) 746.
- [58] Y.J. Uemura, Bose-Einstein to BCS Crossover Picture for High- T_c Cuprates, *Physica C* 282-287 (1997) 194.
- [59] Y.J. Uemura, What can we learn from comparison between cuprates and He Films?: Phase separation and actuating superconductivity, *Int. J. Mod. Phys. B* 14 (2000) 3003.
- [60] Y.J. Uemura, Microscopic phase separation in the overdoped region of high- T_c cuprate superconductors, *Solid State Commun.* 120 (2001) 347.
- [61] S.H. Pan, J.P. O'Neal, R.L. Badzey, C. Chamion, H. Ding, J.R. Engelbrecht, Z. Wang, H. Eisaki, S. Uchida, A.K. Gupta, W.-W. Ng, E.W. Hudson, K.M. Lang, J.C. Davis, Microscopic electronic inhomogeneity in the high- T_c superconductor $\text{Bi}_2\text{Sr}_2\text{CaCu}_2\text{O}_{8+x}$, *Nature* 413 (2001) 282.
- [62] G. Agnolet, D.F.M. Cooley, J.D. Reppy, Kosterlitz-Thouless Transition in Helium Films, *Phys. Rev. B* 39 (1989) 8934.
- [63] D.J. Bishop, J.E. Berthold, J.M. Parpia, J.D. Reppy, Superfluid Density of Thin ^4He Films Adsorbed on Porous Vycor Glass, *Phys. Rev. B* 24 (1981) 5047.
- [64] K. Shirahama, M. Kubota, S. Ogawa, N. Wada, T. Watanabe, Size-dependent Kosterlitz-Thouless Superfluid Transition in Thin ^4He Films Adsorbed on Porous Glasses, *Phys. Rev. Lett.* 64 (1990) 1541.
- [65] P.A. Crowell, F.W. Van Keuls, J.D. Reppy, Onset of Superfluidity in ^4He Films Adsorbed on Disordered Substrates, *Phys. Rev. B* 55 (1997) 12620.
- [66] H. Chyo and G.A. Williams, Superfluid Phase Transition of ^3He - ^4He Mixture Films Adsorbed on Alumina Powder, *J. Low Temp. Phys.* 110 (1998) 533.
- [67] M. Chan, N. Mulders, J. Reppy, Helium in Aerogel, *Physics Today* (August, 1996) 30.
- [68] S.A. Kivelson, G. Aeppli, V.J. Emery, Thermodynamics of the interplay between magnetism and high-temperature superconductivity, *Proc. Nat. Acad. Sci.* 98 (2001) 11903.
- [69] M. Matsuda, M. Fujita, K. Yamada, R.J. Birgeneau, M.A. Kastner, H. Hiraka, Y. Endoh, S. Wakimoto, G. Shirane, Static and dynamic spin correlations in the spin-glass phase of slightly doped $\text{La}_{2-x}\text{Sr}_x\text{CuO}_4$, *Phys. Rev. B* 62 (2000) 9148.
- [70] G.S. Boebinger, Y. Ando, A. Passner, T. Kimura, M. Okuya, J. Shimoyama, K. Kishio, K. Tamasaku, N. Ichikawa, S. Uchida, Insulator-to-Metal Crossover in the Normal State of $\text{La}_{2-x}\text{Sr}_x\text{CuO}_4$ Near Optimal Doping, *Phys. Rev. Lett.* 77 (1996) 5417.
- [71] B. Lake, G. Aeppli, K.N. Clausen, D.F. McMorrow, K. Lefmann, N.E. Hussey, N. Mangkomtong, M. Nohara, H. Takagi, T.E. Mason, A. Schroder, Spins in the Vortices of High-Temperature Superconductor, *Science* 291 (2001) 1759.
- [72] E. Dagotto, T. Hotta and A. Moreo, Colossal Magnetoresistant Materials: The Key Role of Phase Separation, *Phys. Rep.* 344 (2001) 1.
- [73] M. Matsuda, M. Fujita, K. Yamada, R.J. Birgeneau, Y. Endoh, G. Shirane, Electronic Phase Separation in Lightly-doped $\text{La}_{2-x}\text{Sr}_x\text{CuO}_4$, arXiv cond-mat/011228.
- [74] M.J. Larkin, A. Kinkhabwala, Y.J. Uemura, Y. Sushko, G. Saito, Pressure dependence of the magnetic penetration depth in $-(\text{BEDT-TTF})_2\text{Cu}(\text{NCS})_2$, *Phys. Rev. B* 64 (2001) 144514.
- [75] Y.J. Uemura, A. Keren, G.M. Luke, L.P. Le, B.J. Sternlieb, W.D. Wu, J.H. Brewer, R.L. Whetten, S.M. Huang, Sophia Lin, R.B. Kaner, F. Diederich, S. Donovan, G. Gerner, K. Holzer, Magnetic Field Penetration Depth in K_3C_{60} Measured by Muon Spin Relaxation, *Nature* 352 (1991) 605.
- [76] Y.J. Uemura, A. Keren, L.P. Le, G.M. Luke, W.D. Wu, J.S. Tsai, K. Tanigaki, K. Holzer, S. Donovan, R.L. Whetten, System Dependence of the Magnetic Field Penetration Depth in C_{60} Superconductors, *Physica C* 235-240 (1994) 2501.
- [77] H. Amitsuka, M. Sato, N. Metoki, M. Yokoyama, K. Kuwahara, T. Sakakibara, H. Morimoto, S. Kawarazaki, Y. Miyako, J.A. Mydosh, Effect of Pressure on Tiny Antiferromagnetic Moment in the Heavy-Electron Compound URu_2Si_2 , *Phys. Rev. Lett.* 83 (1999) 5114.
- [78] K. Matsuda, Y. Kohori, T. Kohara, K. Kuwahara, H. Amitsuka, Spatially Inhomogeneous Development of Antiferromagnetism in URu_2Si_2 : Evidence from ^{29}Si NMR under Pressure, *Phys. Rev. Lett.* 87 (2001) 087203.
- [79] G.M. Luke, A. Keren, L.P. Le, Y.J. Uemura, W.D. Wu, D. Bonn, L. Taillefer, J.D. Garrett, Y. Onuki, Muon Spin Relaxation in Heavy Fermion Systems, *Hyperne Interact.* 85 (1994) 397.
- [80] Y.J. Uemura, W.J. Kossler, X.H. Yu, H.E. Schone, J.R. Kempton, C.E. Stronach, S. Barth, F.N. Gyagax, B. Hitti, A. Schenck, C. Baines, W.F. Lankford, Y. Onuki, T. Komatsubara, Coexisting Static Magnetic Order and Superconductivity in $\text{CeCu}_{2.1}\text{Si}_2$ Found by Muon Spin Relaxation, *Phys. Rev. B* 39 (1989) 4726.
- [81] G.M. Luke, A. Keren, K. Kojima, L.P. Le, B.J. Sternlieb, W.D. Wu, Y.J. Uemura, Y. Onuki, T. Komatsubara, Competition between Magnetic Order and Superconductivity in $\text{CeCu}_{2.2}\text{Si}_2$, *Phys. Rev. Lett.* 73 (1994) 1853.
- [82] P. Chandra, P. Coleman, J.A. Mydosh, Pressure-induced Magnetism and Hidden Order in URu_2Si_2 , cond-mat/0110048.

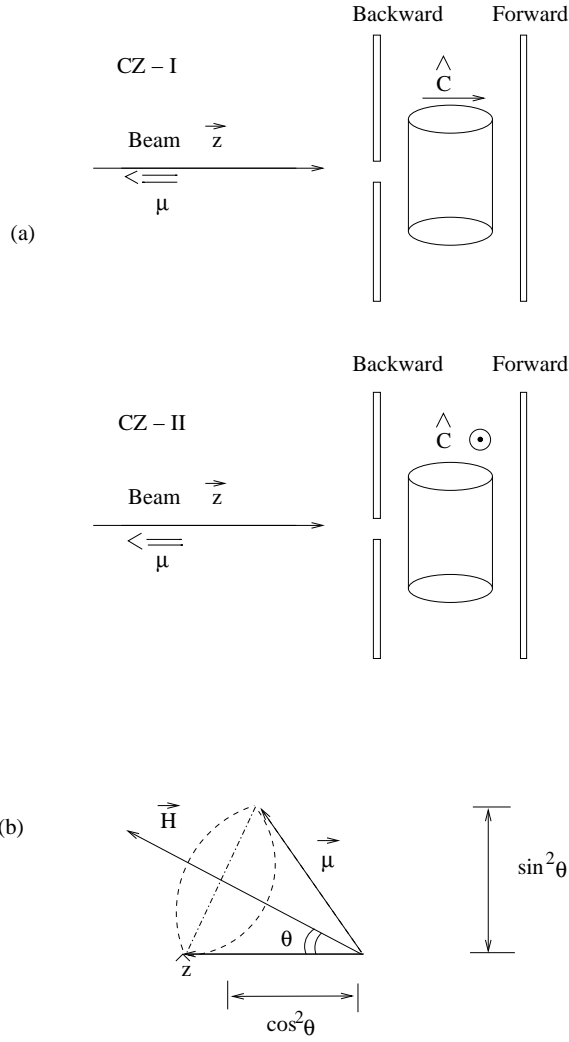


FIG. 1. (a) Schematic view of the experimental configurations in zero field SR (ZF-SR) employed in the present study. Measurements were performed with the initial muon spin polarization parallel (CZ-I) and perpendicular (CZ-II) to the \hat{c} -axis, by rotating the crystal orientation by 90 degrees. The upper [lower] figure shows the CZ-I [CZ-II] configuration. (b) Illustration of the oscillating part of the muon polarization signal, proportional to $\sin^2(\theta)$, with θ being the angle between the local magnetic field and the initial muon spin direction. The $\cos^2(\theta)$ component contributes to the amplitude of the non-oscillating signal.

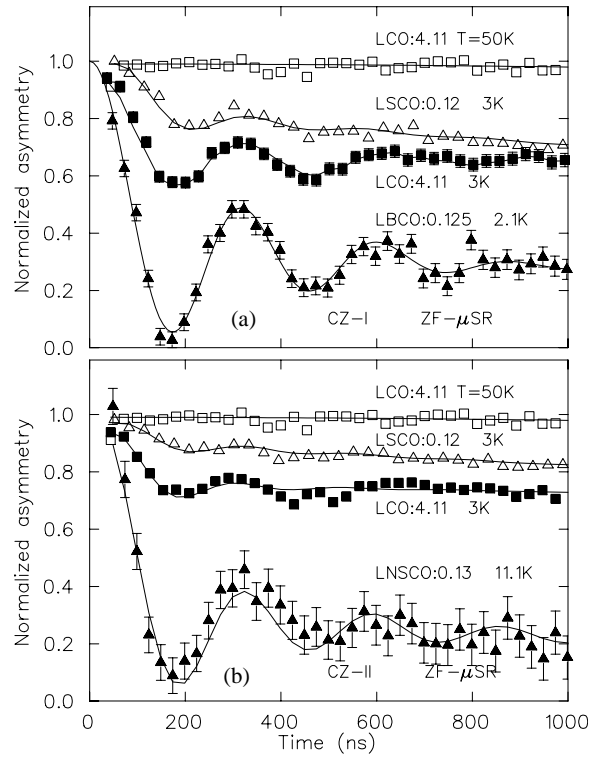


FIG. 2. Time spectra of the muon spin polarization observed by ZF-SR with (a) the CZ-I configuration, and (b) the CZ-II configuration for $\text{La}_2\text{CuO}_{4.11}$ (LCO:4.11) and $\text{La}_{1.88}\text{Sr}_{0.12}\text{CuO}_4$ (LSCO:0.12). Also included are results for ceramic specimens of $\text{La}_{1.875}\text{Ba}_{0.125}\text{CuO}_4$ (LBCO:0.125) from [36] and $\text{La}_{1.47}\text{Nd}_{0.4}\text{Sr}_{0.13}\text{CuO}_4$ (LNSCO:0.13) from [38].

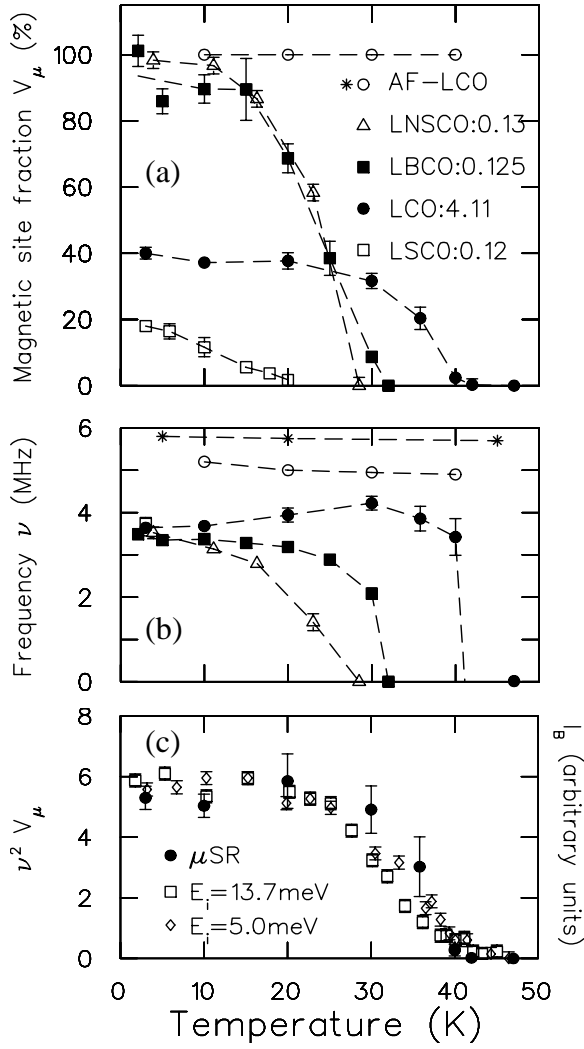


FIG. 3. (a) Volume fraction V of muon sites with a static magnetic field larger than 30 G and (b) frequency of the precessing signal in $\text{La}_2\text{CuO}_{4.11}$ (LCO :4.11) and $\text{La}_{1.88}\text{Sr}_{0.12}\text{CuO}_4$ (LSCO :0.12) (from the present study), compared with the results in $\text{La}_{1.875}\text{Ba}_{0.125}\text{CuO}_4$ (LBCO :0.125) [36], $\text{La}_{1.47}\text{Nd}_{0.4}\text{Sr}_{0.13}\text{CuO}_4$ (LNSCO :0.13) [38], and antiferromagnetic $\text{La}_2\text{CuO}_{4+}$ (AF-LCO) [27,28]. The broken lines are guides to the eye. (c) Comparison of the temperature dependence of the Bragg peak intensity I_B of neutron scattering measurements in $\text{La}_2\text{CuO}_{4.11}$ (LCO :4.11) [16] with those expected from the SR results (present study) as I_B / V^2 . SR and neutron results are scaled using the values near $T \rightarrow 0$. Comparison of the absolute values is discussed in Section V-B.

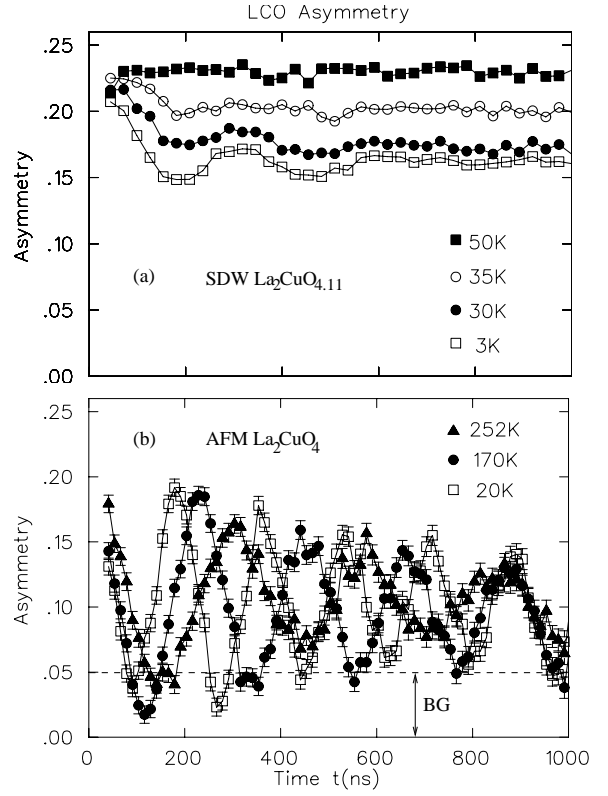


FIG. 4. Time spectra of ZF-SR measurements in (a) LCO :4.11 and (b) AF-LCO, at various temperatures. The amplitude of the oscillating and relaxing signal varies in (a) below T_N without much change in the frequency, while in (b) the amplitude does not depend on T and the frequency increases with decreasing T . The latter behavior is observed in ZF-SR of many conventional magnetic systems. The spectrum (a) was obtained by using low-background SR spectrometer, which ensures that the background signal level is below 0.01 in Asymmetry. The spectrum (b) was obtained in 1987 by using older apparatus. The broken line (BG) indicates an expected level of background signal in (b).

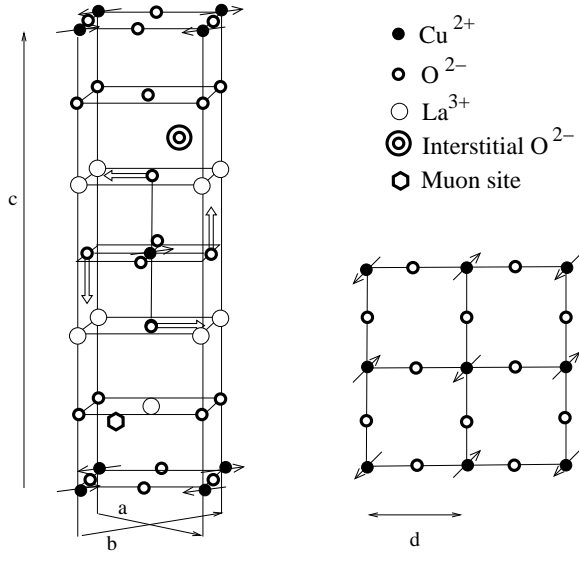


FIG. 5. Schematic view of the crystal structure of La_2CuO_4 , shown with the positions of intercalated interstitial oxygen and the muon site associated with an apical oxygen. We assume the location of muon site near apical oxygen to be $(0,0.751,2.257)$ Å within the unit cell. The arrows attached to O^{2-} in the center of the figure show the direction of tilting (about 5°) of the CuO_6 octahedra.

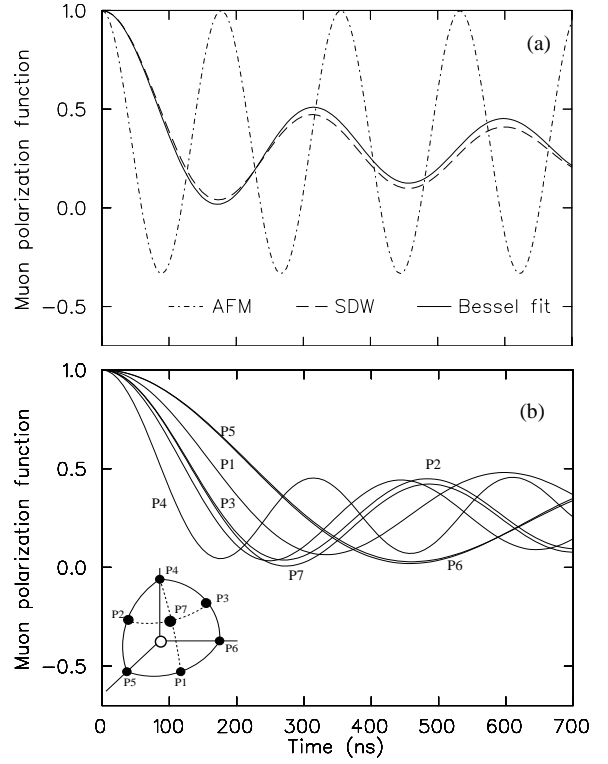


FIG. 6. Computer simulation results of the muon spin polarization functions expected for La_2CuO_4 assuming that all the Cu moments involved in the static magnetic order. An angular average is taken to represent the results for ceramic specimens. (a) Results for the muon site near the apical oxygen (see Fig. 5). The dotted line corresponds to the case with antiferromagnetic (AFM) spin correlations with the static Cu moment of $0.55 \mu_B$, while the dashed line corresponds to the case with spin density wave (SDW) amplitude modulation with maximum static Cu moment of $0.35 \mu_B$ and modulation wavevector $k = 0.12 \pi/d$ ($d = 3.779 \text{ Å}$) superimposed on the antiferromagnetic correlations. The solid line is the result of a fit to a Bessel function. (b) Results for several hypothetical muon sites near the intercalated interstitial oxygen, illustrated in the inset, obtained for the above-mentioned SDW spin correlations.

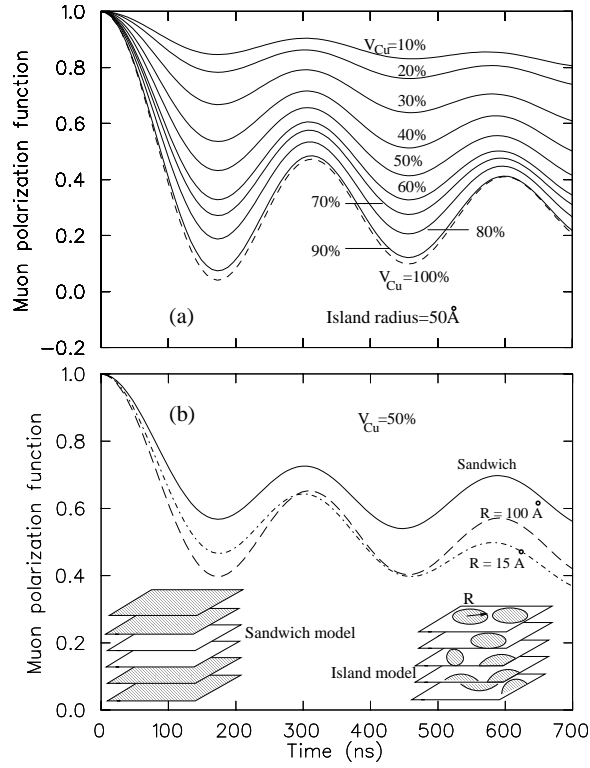


FIG. 7. Computer simulation results of the expected muon spin polarization functions for La_2CuO_4 , with only a part of the Cu moments involved in the static magnetic order, obtained for the muon site near the apical oxygen after angular average to simulate the results for ceramic specimens. We assume a SDW modulation with a maximum static Cu moment of $0.35 \mu_B$ and modulation vector $k = 0.12 \pi = d$. (a) Magnetic island model where the Cu moments in a volume fraction V_{Cu} order with the SDW amplitude modulation, forming islands of radius $R = 50$ Å. (b) Comparison of the results for the magnetic island model with $R = 15$ and 100 Å with those for the "sandwich model" where two CuO_2 planes adjacent to the intercalated oxygen layer do not have any static Cu moments while all the Cu moments on the other two planes are ordered. All three curves shown in (b) correspond to $V_{Cu} = 50\%$. The insets illustrate these two models, with the shaded regions containing SDW modulated static Cu moments and the blank regions without static Cu moments.

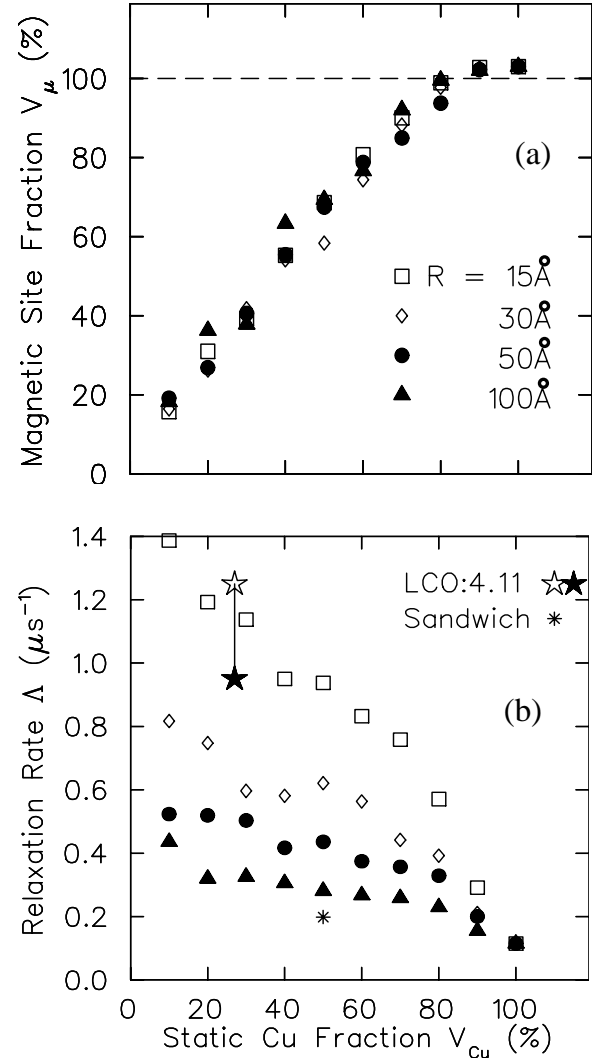


FIG. 8. (a) Computer simulation results for the volume fraction V of muon sites with a static magnetic field larger than ~ 30 G as a function of the volume fraction of the sample containing static Cu moments, V_{Cu} . (b) The relaxation rate of the Bessel function oscillation, obtained by fitting the simulation results with Eq. 3, plotted as a function of V_{Cu} . Comparison with the experimental results for LCO:4.11 (Raw data 4.11 shown by an open star symbol and corrected data 4.11 by a closed star symbol) allows estimation of the size of magnetic islands. The asterisk symbol * shows the relaxation rate expected for the sandwich model.

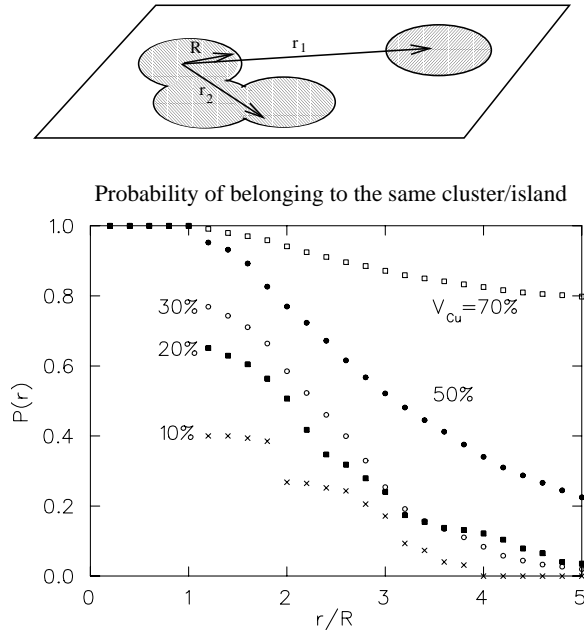


FIG .9. Probability $P(r)$ that Cu spins belong to a certain cluster versus the distance from the center of an of radius R in the cluster. We assume that all the spins in a given island are correlated, and the correlation extends if there is any small overlap between adjacent islands on a given CuO_2 plane, as illustrated in the upper figure. For example, a Cu spin at a distance r_2 contributes "1.0" for the probability, while that at r_1 gives "0.0" contribution. We average over all the possible cluster/island configurations to calculate $P(r)$. The results demonstrate a long length scale of spin correlations for the "magnetic island model", due to formation of large clustered islands.

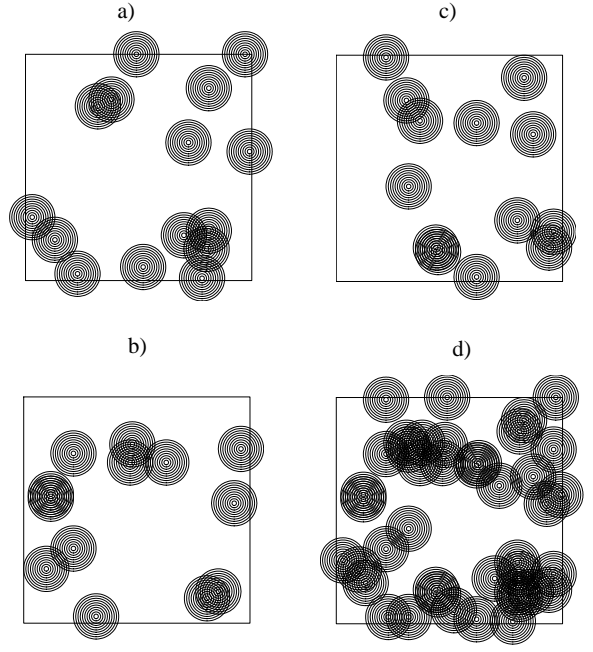


FIG .10. Illustration of percolating cluster islands. (a)-(c) show planes with random locations of magnetic islands having integrated area fraction of 30%. (d) shows the overlap of (a)-(c). (d) demonstrates that most of the islands belong to the percolating cluster if we allow correlations of spins in "overlapping islands" on all the three planes.

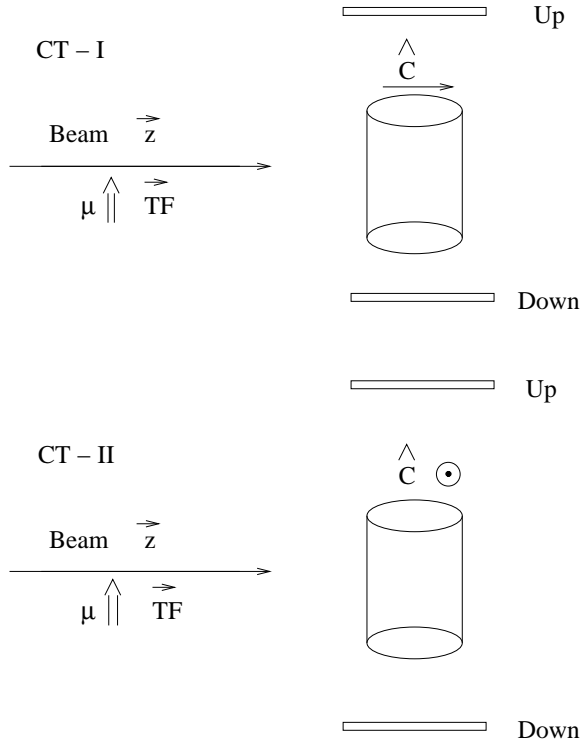


FIG. 11. Schematic view of experimental configurations of Transverse Field SR (TF-SR) measurements employed in the present work with the external field applied parallel (CT-I) and perpendicular (CT-II) to the \hat{c} -axis of the single crystal.

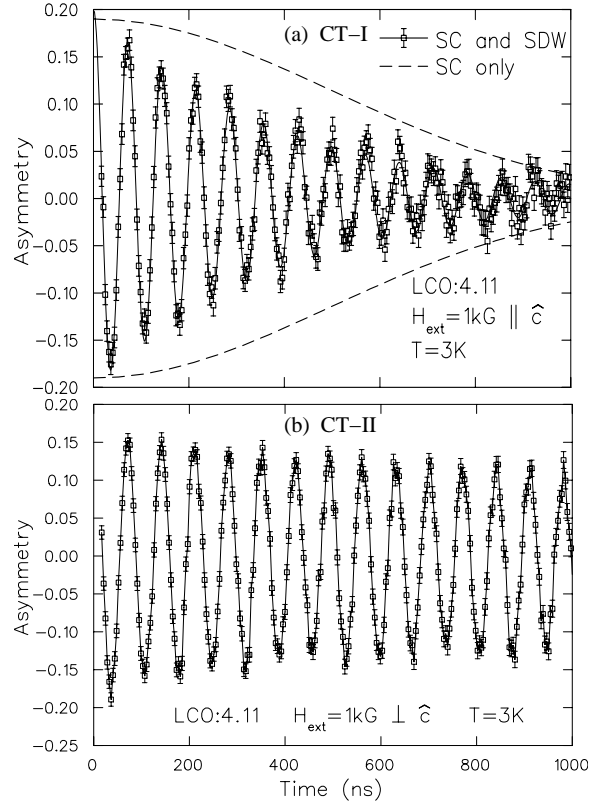


FIG. 12. Time spectra of the muon spin polarization observed in TF-SR in LCO 4.11 obtained using (a) CT-I and (b) CT-II configurations. The relaxation of the signal is due to a distribution of magnetic fields inside a superconducting sample (SC) and magnetic fields due to static Cu moments with the SDW amplitude modulation. (a) shows faster damping than (b), reflecting the shorter penetration depth for the external field applied perpendicular to the CuO_2 planes. The expected effect from superconductivity alone is shown by the dotted line in (a).

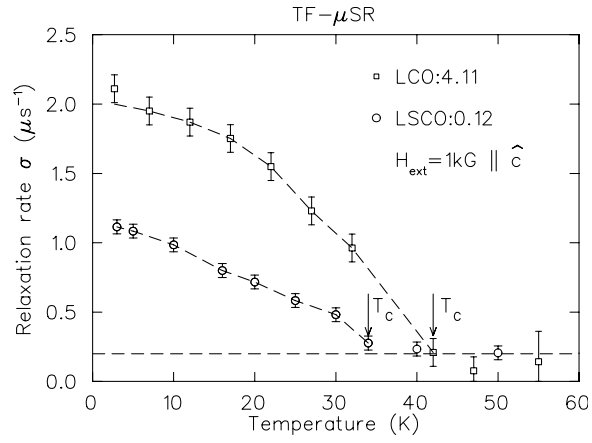


FIG. 13. Temperature dependence of the superconducting relaxation rate due to superconducting flux vortices, observed in TF- μ SR measurements (with the CT-I configuration) in $\text{La}_2\text{CuO}_{4.11}$ (LCO:4.11) and $\text{La}_{1.88}\text{Sr}_{0.12}\text{CuO}_4$ (LSCO:0.12). The broken lines are guides to the eye.

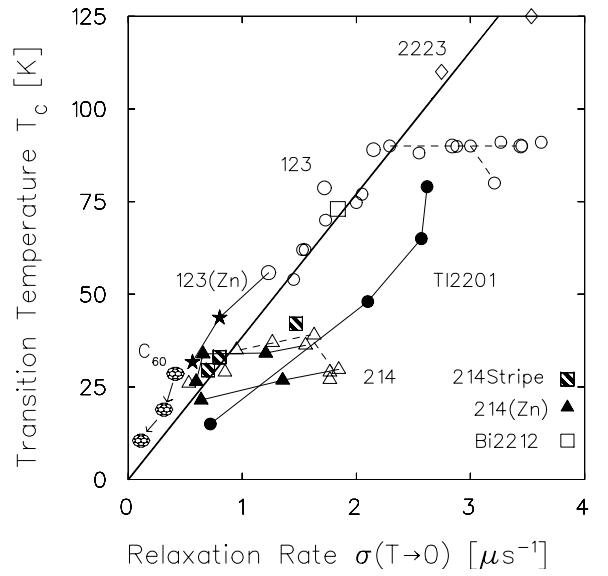


FIG. 14. A plot of the superconducting transition temperature T_c versus the relaxation rate ($T \rightarrow 0$) at low temperatures (proportional to the superfluid density n_s/m) for several high- T_c superconductors [49–52]. The results with the “stripe square” symbols represent points from LESCO ([54,55]), LSCO 0.12, and LCO 4.11 in the order of increasing ($T \rightarrow 0$). To account for difference between results for ceramic and single-crystal specimens, the values for LCO 4.11 and LSCO 0.12 in the CT-I configuration were multiplied by 1/1.4.

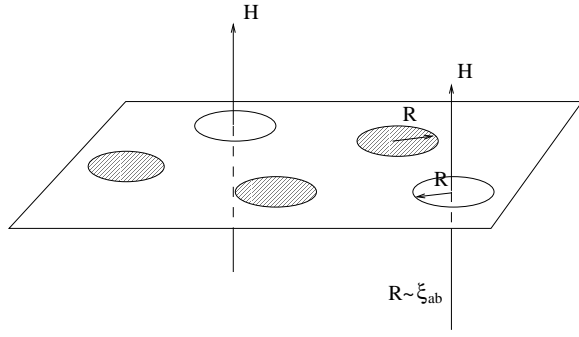


FIG. 15. An illustration of magnetic islands (shaded circles) and vortex cores (open circles) on the CuO_2 planes of HTSC systems under an external magnetic field applied along the c axis direction. When a core is located at the magnetic island, one expects an increase in the radius of the non-superconducting region due to supercurrent flowing around such a magnetic island.